ARCHIVES OF METALLURGY AND MATERIALS
Volume 51 2006 Issue 1

K. SZTWIERTNIA*, M. BIEDA*, G. SAWINA*

DETERMINATION OF CRYSTALLITE ORIENTATIONS USING TEM. EXAMPLES OF MEASUREMENTS

WYZNACZANIE ORIENTACJI KRYSTALITÓW W TEM. PRZYKŁADY POMIARÓW

Determination of topography of crystallite orientations becomes important technique of investigation of polycrystalline materials. Electron back- scattered diffraction (EBSD) in scanning electron microscopy (SEM) is already extensively used for creating orientations maps. Recently, transmission Kikuchi patterns (TKP) as well as convergent beam electron diffraction patterns (CBED) in transmission electron microscope (TEM) have been applied for creating such maps. The paper presents exemplary results of measurements of local crystallographic orientations in highly cold- rolled aluminium as well as in aluminium alloy 6013. For determination of crystallite orientations the software *EP*, developed by Morawiec, Funderberger, Bouzy and Lecomte [1–5], was used. The TKP and CBED patterns for EP were obtained by scanning of conventional photographic plates from TEM.

Wyznaczanie topografii orientacji krystalograficznych stało się ważną technika badania materiałów polikrystalicznych. Do tworzenia map orientacji wykorzystuje się powszechnie technikę wykorzystującą dyfrakcję elektronów wstecznie rozproszonych (EBSD) w skaningowych mikroskopach elektronowych. Ostatnio do tworzenia tego typu map zastosowano obrazy dyfrakcyjne Kikuchiego (TKP) oraz obrazy dyfrakcyjne uzyskane przy użyciu wiązki zbieżnej (CBED) w transmisyjnym mikroskopie elektronowym (TEM). W pracy przedstawiono przykładowo wyniki pomiaru lokalnych orientacji krystalograficznych w walcowanych na zimno do wysokich stopni zgniotu czystym aluminium i stopie aluminium 6013. Dla określenia orientacji krystalitów wykorzystano program opracowany przez Morawca, Funderberger'a, Bouzy'iego i Lecomte'a [1–5]. Obrazy TKP lub CBED dla EP ze zdefiniowanych miejsc próbki zostały otrzymane przez skanowanie konwencjonalnych klisz fotograficznych z TEM.

1. Introduction

Development of new materials is influenced by progress in microstructure characterization. The introduction of a new generation of computer controlled electron microscopes allows obtaining very detailed and statistically significant information for the quantitative description of microstructure at the highest possible spatial resolution. Such a description can base on crystallographic orientations acquired from systematical local measurements in the sample space called orientation mapping (OM). OM may be used for quantitative description of microstructure of each polycrystalline material. The following orientation characteristics of microstructure can be determined: orientation distribution functions (textures), misorientation distribution functions (the distributions characterize boundaries between grains of one or different phases), as well as the so-called partial distribution functions defined for sets of orientations after appropriate selection [e.g. 6]. OM techniques can be used for quick phase identification. The knowledge of orientations topography allows one to identify subgrain boundaries and other heterogeneities on the basis of a selection of misorientations between neighbouring measurement points; therefore, it is possible to carry out stereological analysis that takes into account crystallographic orientation. The additional data contained in the diffraction image can also be used, e.g. for differentiation of material areas with different dislocation density.

At present, due to the progress in the automation of the diffraction measurements, especially in the SEM (SEM/FEG, ESEM), it is easy to carry out routine fast orientation measurements. However, spatial resolution obtained in this case is often not sufficient for investigation of extremely fine-grained or highly deformed

* INSTITUTE OF METALLURGY AND MATERIALS SCIENCE, POLISH ACADEMY OF SCIENCES, 30-059 KRAKÓW, 25 REYMONTA ST., POLAND

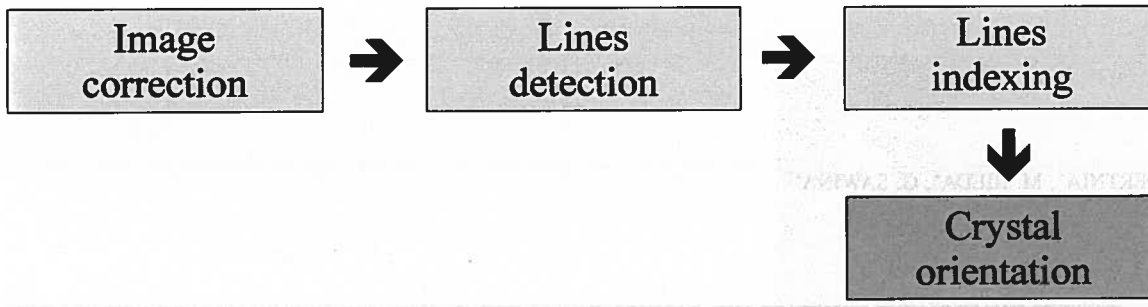

Fig. 1. The diagram illustrating the operation of the program *Ep*

materials. It is the ground that the techniques of OM are also developed in TEM [e.g. 1–4, 7, 8]. The transition from SEM measurements on metallographic specimens to TEM measurements on thin foils improves about 100 times the resolution capability, i.e. it allows obtaining data from areas of several nanometres.

2. Local crystallographic orientations measurement in TEM

For the measurement of local crystallographic orientations the program *EP* has been used [1–3, 4]. *EP* could indexing TKP and CBED patterns and is general; it can be applied to any crystal structure. The program is designed to work in a system with a digital camera attached to the microscope. However, if TEM is not equipped with an appropriate camera, the measurement of local crystallographic orientations with help of the *EP* is still possible. Diffraction pattern from the defined foil point may be recorded on photographic plate and then scanned to obtain its digital version (e.g. in the form of bitmap). Series of bitmaps may be analyzed by the *EP* program. Then sets of orientations produced by *EP* may be processed by a number of other, specialized programs, used to calculate functions defined on orientations or misorientations [e.g. 6].

2.1. EP programme structure

The prototype system of *EP* software, covering automatic detection of lines pairs in diffraction patterns and automatic indexing of them, was prepared by Morawiec [1] in cooperation with LETAM, University of Metz, where elements of the system interface were developed [1–3]. Fig. 1 presents the principle elements of *EP* software system.

2.2. Correction, detection of lines and indexing of the diffraction pattern

As mentioned before, *EP* allows diffraction patterns to be loaded from bitmap files, which are recorded, either directly — by means of a digital camera, or indirectly — by processing analogue photographic film. In the first step of processing *EP* corrects (background elimination included) the digital images. Fig. 2a shows a diffraction pattern of relatively good quality after correction. In the

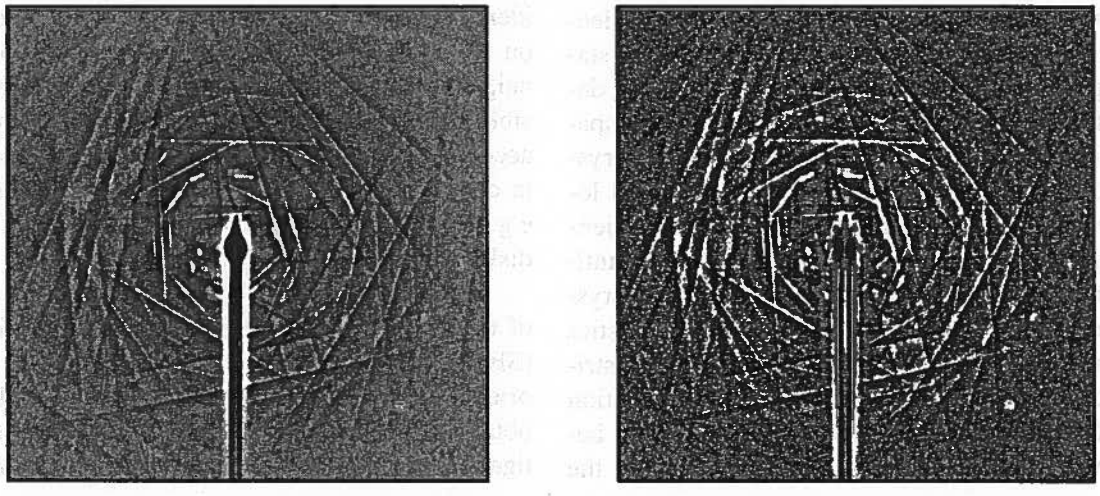

Fig. 2. a) The output diffraction image after background elimination, b) The image with enhanced lines

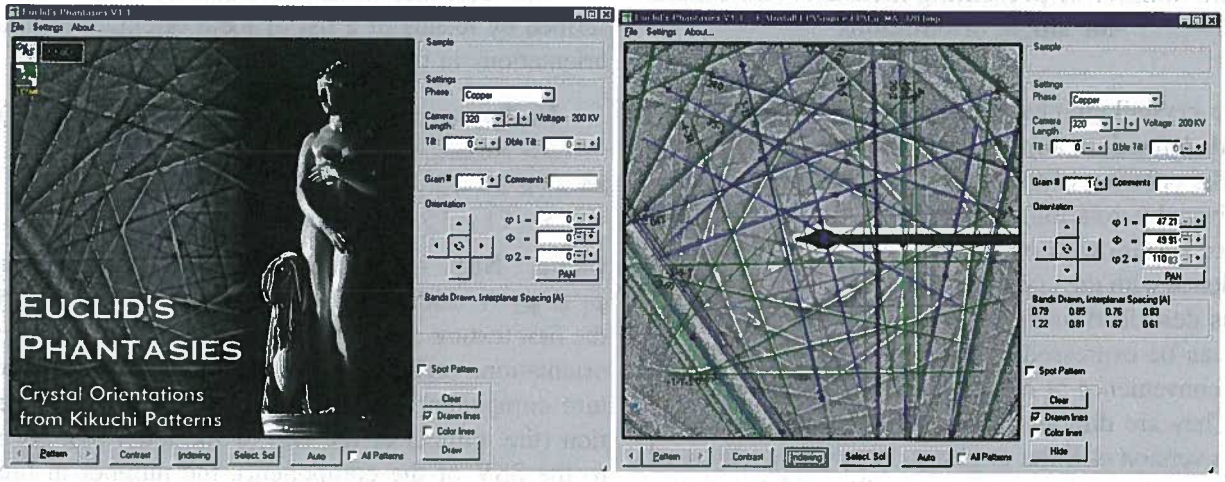

Fig. 3. The dialog box of *EP* software that allows one to introduce lines manually (blue lines — indicated manually, green lines — simulated image)

second step *EP* detects lines. The automatic line detection is based on the Hough transform. However, such a standard line detection procedures applied directly to even good quality images like this in Fig. 2a does not yield satisfactory results. Therefore, *EP* includes routines aimed at enhancing lines and transforming histogram image that improve detection efficiency. Fig. 2b shows a typical image obtained by the implementation of one of the selected procedures. Image segmentation turned out to be an efficient method of reducing the impact of noise, point image traces and artefacts created by background elimination.

In the last step of line detection, the lines are joined into pairs.

Then the lines are indexed. The indexing procedure is to match the points of the reciprocal lattice calculated from the crystallographic data and the lattice points obtained from the measured diffraction pattern. The orientation is obtained by calculating the rotation transforming the first set onto the second one in such a way that the discrepancy between the sets after the rotation takes its minimum. The principles of pattern indexing and orientation determination procedures are described by Morawiec [4].

2.3. EP programme operation

The software operation may be divided into 4 steps:

1) Setting TEM microscope operation parameters — „Settings" field.
2) Input of crystallographic data. New data are added by clicking „New Phase" in „File" menu. Details can be found in software documentation [5].
3) Reading a set or single diffraction image („Pattern" button).
4) Indexing of diffraction images.

Indexing can be realized automatically and manually. The first consists in using „Auto" button. The program shall automatically identify and index all indicated in the particular set diffraction patterns. In some cases of poor quality diffraction, it is not always possible to correctly identify diffraction lines automatically. Then, Kikuchi lines may be indicated „manually". After marking several pairs (from 3 to 10), one may solve diffraction by pressing 'Indexing' button. The 'Orientation' field shall display the calculated orientation.

3. The use of local, crystallographic orientation measurements in microstructure analysis

EP software was used to calculate orientation from TKP and CBED patterns registered on photographic plates in pure aluminium and in 6013 aluminium alloy cold-rolled to 75% and 90%. Orientations were measured along the selected sample directions. The investigations were carried out within the framework of a larger project, aimed at comparing the growth mechanisms of recrystallization nuclei / new grains in pure aluminium and in the alloy with bimodal distribution of particles of other phases [e.g. 9, 10]. The examination of as-deformed microstructure was carried out by means of TEM (Philips CM 20). Thin foils were prepared primarily from the plane perpendicular to transverse direction TD. Microstructure areas were registered in the bright field, which was followed by the measurement of orientations in these areas. The error of a single measurement in the microscope reference system was smaller than 1°, and smaller than 3° in the sample reference system.

3.1. The manner of presenting measurement results for single orientations

The crystallographic orientation is a feature of the material defined at any point (x,y,z) of the sample at which the ordering of the crystal lattice is not disturbed. It is given by rotation, which bring the local sample reference system with its origin at the point (x,y,z) into coincidence with the crystal reference system. The orientation is described unambiguously by three parameters, which can be expressed in different ways [11]. Usually, for the convenience of calculations, Euler angles are applied. They are differently defined but traditionally, the Bunge's version of Euler angles φ_1, Φ, φ_2 is mostly used. In some problems, the parameters υ, Ψ, ω of the rotation axis (υ, Ψ) and the rotation angle ω are used as easiest to visualize. If an orientation is described by a greater number of parameters, then the parameters depend on each other. Such is the situation in the case of crystallographic indices {hkl}<uvw>, commonly used in practice. In the paper each orientation was described by Bunge's version of Euler angles; additionally the name of the texture component closest to the measured orientation was given. The orientation was identified with the particular component (Table 1), when the disorientation [1] angle between them was smaller than 15°. In the case of rolled to high degrees of deformation polycrystalline sheet, the sample axes parallel to the normal (ND), transverse (TD) and rolling directions (RD) can be interchanged according to orthorhombic symmetry of a sample. Thus each x component is represented by its sample symmetry related variants (SSV). In the paper SSVs are numbered x1, ..., x4; the basic variant and three other generated by the two-fold axes, L^2_{ND}, L^2_{TD}, L^2_{RD}, respectively. It must be noted that the induced by the rolling process sample symmetry has a statistical character, while the crystallites orientations symmetrically equivalent due to this symmetry define their different physical positions. The cubic symmetry of the aluminium crystalline lattice is of physical character and symmetrically equivalent orientations — due to this symmetry — are physically identical.

For neighbouring crystallites, the disorientations in rotational parameters υ, Ψ, ω_d are given. After rotation by angle ω_d, the reference system of the first crystallite is transformed into the reference system of the second crystallite, while the rotation by angle $-\omega_d$ transforms the reference system of the second crystallite into that of the first one. When the appropriate order of crystallite reference systems is maintained, it is possible to examine the phenomenon of disorientation accumulation.

The essential microstructure elements were described by means of a list of local orientations and disorientations in the following form:

No.1$\varphi_1\phi\varphi_2$ **variant A** (ω_{min}) **variant B** (ω_{min})
>> **No2**ω_d, υ, Ψ **[uvw]** (α)
84 334. 37. 75. Brass_Y153(3.9)Brass____**4**(12.9)
>> 71 – 15.4 11.6 36.0[117](1.8)Σ25

where: **No1** — orientation identification number, φ_1 ϕ φ_2 — Euler angles, **variant A** — the symbol of the first texture component variant close to the measured orientation, **variant B** — the symbol of the second texture component variant close to the measured orientation (the number at the end of the letter symbol refers to the SSV of the component), the number in brackets (ω_{min}) refers to the disorientation between the measured orientation and the corresponding SSV of the particular component; >> **No.2** — the number identifying the orientation with respect to which the disorientation is given (if missing, the disorientation is given with respect to the next orientation), ω_d — misorientation angle, υ, Ψ — polar coordinates of the rotation axis, **[uvw]** — rotation axis indexes close to the calculated axis, (α) — the angle between the calculated axis and **[uvw]**; **Σ** — the coincidence degree (only in the case, when the disorientation fulfilled Brandon's condition for the particular coincidence site lattice (**CSL**) orientation relationship. In the above example, orientation 84 is disoriented from the third variant of Brass_Y + 15 component (Brass rotated around RD by 15° by 3.9° and by 12.9° from the fourth variant of Brass component; and the disorientation between the crystallite 84 and the crystallite 71 can be described as rotation by –15.4° around the rotation axis ~[117], which corresponds to CSL relation with Σ = 25.

3.2. Rolled aluminium — deformed state

Aluminium, cold rolled to 90%, has shown the deformation texture of the copper type with β and α fibres. In the main fibre β, components S, Copper, R_Brass, and in fibre α, components Goss and Brass could be distinguished. Their shares in the texture (orientations having the disorientation angle ω_{min} smaller than 15° with respect to a certain component) were equal to 26%, 11% and 13%, 5% and 11%, respectively [9]. The matrix was formed of layers of sub-grains, lying roughly parallel to the rolling plane (Fig 4 a, b). The thickness of layers with the same type of orientation varied in width from 1 to 10 μm, and the disorientation angles (ω_d) between the neighbouring layers could attain the maximal

[1] The disorientation is the rotation by the angle ω_d with the smallest possible module around an axis common for both crystallites (υ, Ψ) lying in the basic area of the standard triangle [12]

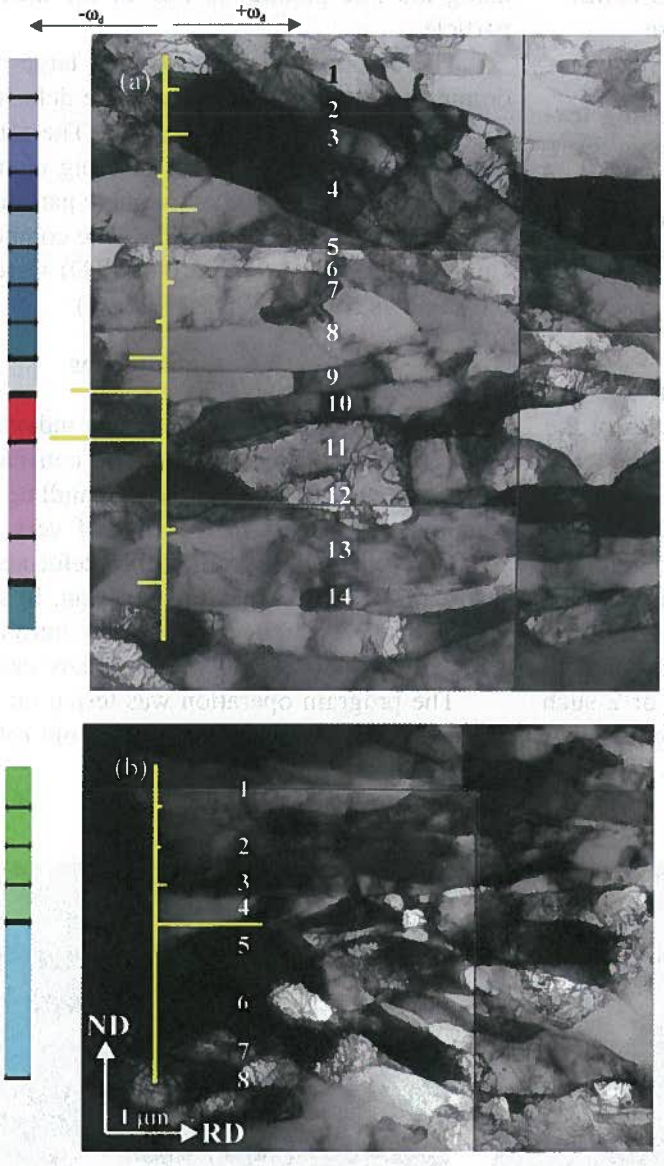

Nr	φ_1	Φ	φ_2	SSV (ω_{min})
	ω	υ	Ψ	
1	179.	25.	64.	Brass1(27.8)
>	5.1	39.0	42.3	
2	168.	25.	76.	Brass1(24.3)
>	8.4	25.9	34.2	
3	160.	32.	85.	Brass1(17.5)
<	-3.0	27.2	21.6	
4	155.	33.	1.	Brass1(15.5)
>	12.0	46.2	32.1	
5	142.	39.	17.	S_4(16.1)
<	-3.4	14.7	21.3	
6	142.	36.	17.	S_4(15.3)
>	3.1	46.0	25.2	
7	142.	33.	15.	S_4(14.6)
<	-2.9	42.4	24.1	
8	138.	32.	19.	S_4(13.4)
<-	12.5	34.0	17.6	
9	149.	28.	20.	RBrass4(19.)
<-	33.7	18.1	1.1	
10	54.	13.	33.	Cube(13.6)
<-	42.9	15.9	3.3	
11	156.	36.	13.	Goss(17.9)
<	-.2	22.9	40.3	
12	157.	36.	12.	Goss(17.7)
>	4.6	19.0	12.1	
13	149.	36.	19.	S_4(22.9)
<-	11.0	54.3	44.5	
14	134.	32.	24.	S_4(13.1)
1	230.	41.	62.	S_2(10.0)
>	3.0	41.8	31.1	
2	228.	42.	66.	S_2(10.2)
>	2.1	26.3	40.6	
3	227.	41.	65.	S_2(11.0)
>	4.8	13.4	20.2	
4	227.	42.	60.	S_2(14.9)
>44	.3	52.0	39.4	
5	287.	39.	36.	S_3(9.0)
<	-.7	42.9	5.5	
6	286.	40.	37.	S_3(9.4)
<	-.9	3.1	23.0	
7	288.	39.	36.	S_3(8.5)
>	.8	3.7	37.9	
8	288.	40.	35.	S_3(8.5)

Fig. 4. Microstructure of 90% cold rolled aluminum, longitudinal section. There are given some orientations (in Euler's angles $\varphi_1, \Phi, \varphi_2$) as well as the orientation relationships (in rotational parameters ω_d, υ, Ψ); letters with numbers indicate the SSVs of the particular component nearest to the measured orientation (numbers in brackets give the angle of disorientation ω_{min} from the particular component). a) Example with the ~Cube oriented subgrains. b) Example with two SSVs of the S-component [9]

values (for cubic symmetry), i.e. 62.8°. It has been found that the disorientation cumulate only along very short distances. In a typical measurement, the orientations oscillated around some local orientation (the sign of the disorientation angle changed on average in every second or third crystallite). The disorientation angles were either small (~70% of the disorientations showed the $\omega_d < 15°$) or large ($\omega_d > 30°$). The subgrains were often cumulated into clusters, containing up to 20 crystallites, and having the same type of orientation; clusters having more than 10 subgrains were always built of at least two of SSVs of this orientation. Thus, a considerable part of high angle grain boundaries could be described by misorientations characterizing the relations between orientations being various SSVs of the same component (e.g. Fig. 4 b). The tendency to form clusters was particularly strong in sub-grains with S orientation; ~75% of crystallites of this orientation appeared in clusters containing from 3 to 15 subgrains, and only ~8% occurred as single ones. Subgrains with orientations other than S occurred as single ones or formed clusters composed of 5 crystallites at the most.

3.3. 6013 aluminium alloy — deformation zones around particles of the second phase

As in the case of pure aluminium, the rolling textures (to 75 and 90% of cold work) of 6013 alloy were dominated by orientations scattered between S and Copper components along β fibre. Brass component dominated along considerably weaker α fibre. A small share of the Cube component was also observed.

The deformation structure was dominated by wavy microbands lying approximately parallel to the rolling plane (Fig. 5). Particularly strong corrugation was observed in the vicinity of large ($1 \div 3\mu m$) particles of the second phase. The large particles break up the lamellar structure and create zones of localized strain.

These zones were intensely examined. Due to the highly localized strain, the measurements of single orientations were very difficult; a lot of diffraction patterns could be resolved only manually. In spite of the difficulties, more then 1000 of orientations were measured in the areas around large particles. An example of 2 such measurement lines is presented in Fig. 5 b. Fig. 6 shows an example of detailed analysis of orientations measured along the line parallel to ND in the area close to the particle.

The deformation zones around large particles were dominated by the orientations of the deformation texture rotated around the TD and/or ND. The rotation may be correlated with the observed bending of microbands in the close neighbourhood of the large particles. Moreover, a considerable share of the TD-Cube component (i.e. the Cube component rotated around TD) were observed in the samples rolled to 75% (Table 1).

3.4. Conclusions

The program *EP* was used for indexing diffraction patterns obtained by scanning of conventional photographic plates. *EP* is capable of handling poorly localized lines. However, in the case of very dizzy images obtained for example from highly-deformed samples the automatic detection may not function. In such cases, an experienced researcher may try to introduce the lines manually. This method works in many cases.

The program operation was tested on pure aluminium and on 6013 aluminium alloy, cold rolled to 75 and 90%, respectively.

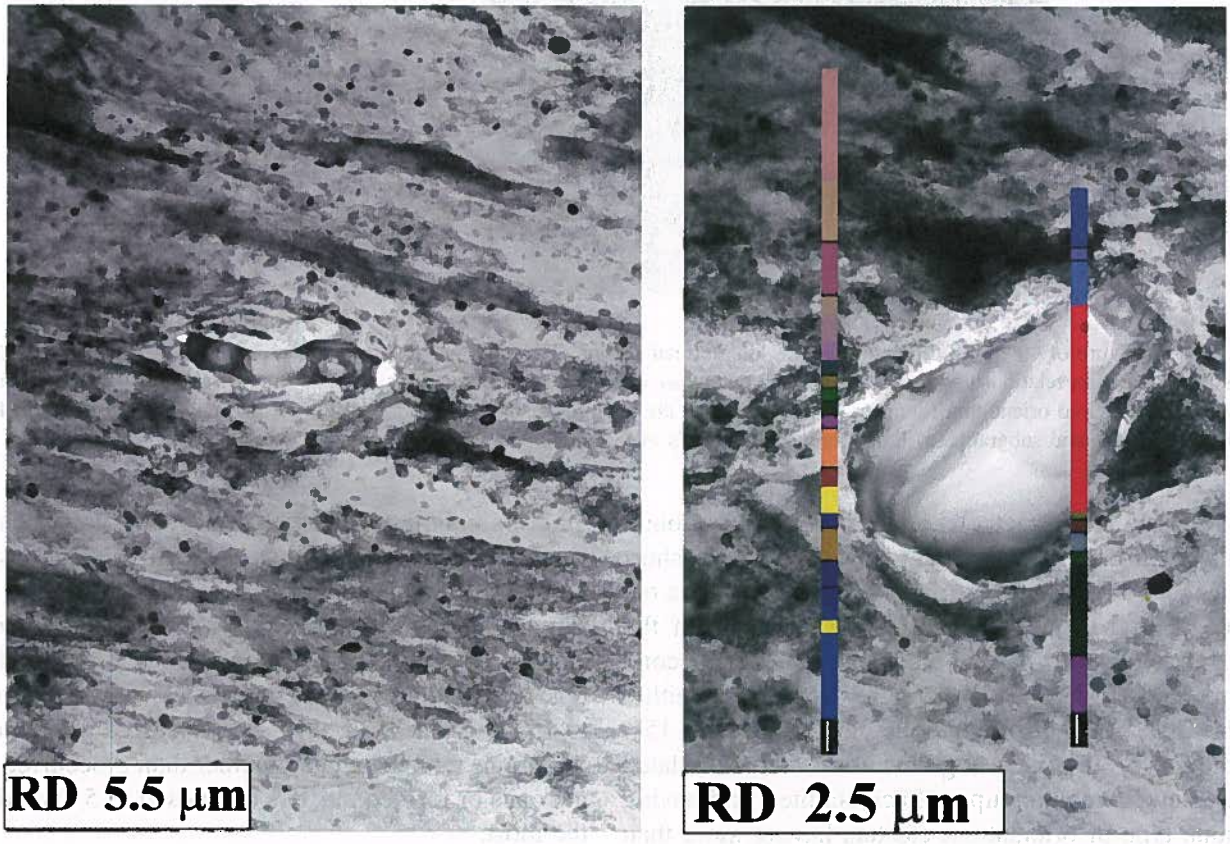

Fig. 5. a) Microstructure of 75% cold rolled 6013 aluminum alloy, longitudinal section, TEM. b) Changes of orientations along 2 lines parallel to ND in the deformation zone around large particle

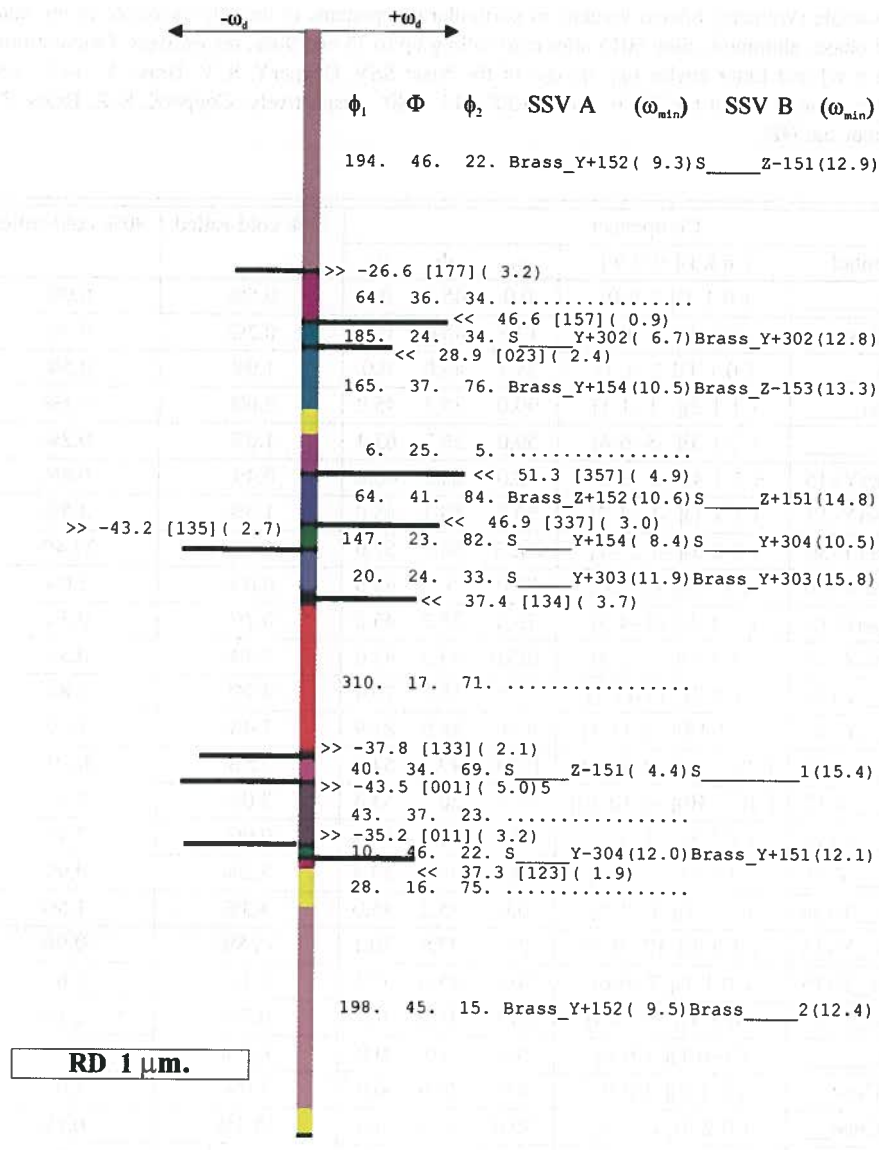

Fig. 6. Microstructure of 75% cold rolled 6013 aluminum alloy. Example of orientation analysis along ND; the neighborhood of the large particle of the second phase

In the case of pure aluminium, the measurement of local crystallographic orientations in TEM did not pose any problems. It was observed that grains divide into smaller fragments during the material deformation. In the case of ~90% deformation, bands with a similar orientation were about 10 μm wide and included eight or nine subgrains. Clusters characterized by one component type, but containing more than 9 subgrains, consisted always of at least two SSVs, which resulted in the appearance of characteristic type of high-angle grain boundaries. Orientation sets measured along ND were used to simulate growth (subgrain thickening) during recrystallization [9].

In the cold rolled 6013 alloy, the examination focused on the areas of localized deformation in the vicinity of large particles of the second phase. The measurements of single orientations in these areas were very difficult. A considerable part of diffraction patterns had to be resolved manually. However, one of the first orientation characteristics of this type of areas was obtained [10]. The examination showed that the areas are dominated by orientations of deformation texture rotated around the TD (and/or ND) by the angles of up to 40°.

Acknowledgements

Financial support from the State Committee for Scientific Research (KBN - 7T08A 054 21) is gratefully acknowledged.

TABLE 1

The fractions [in %] of all sample symmetry related variants of particular components in the sets measured in the deformation zones around large particles of the second phase, aluminum alloy 6013 after cold rolling up to 75 and 90%, respectively. Orientations are given by symbols, the Miller indices (h k l)[u v w] and Euler angles (φ_1, Φ, φ_2) of the basic SSV. CopperY, S_Y, Brass_Y: +15°, +30°, -15°, -30° indicate the particular orientation after rotation about the TD by +15°, +30°, -15°, -30°, respectively; CopperZ, S_Z, Brass_Z indicate the particular orientation after rotation about the ND

Component					75% cold-rolled	90% cold-rolled
Symbol	(h k l)[u v w]	φ_1	Φ	φ_2		
Goss_____	(0 1 1)[1 0 0]	0.0	45.0	0.0	0.5%	0.9%
ND-Goss___	(0 1 1)[6 -1 1]	13.3	45.0	0.0	0.2%	0.7%
Brass_____	(0 1 1)[2 -1 1]	35.3	45.0	0.0	1.9%	0.5%
Copper____	(1 1 2)[-1 -1 1]	90.0	35.3	45.0	2.6%	0.1%
S_____	(2 1 3)[-3 -6 4]	59.0	36.7	63.4	1.6%	0.2%
CopperY+15	(1 1 4)[-2 –2 1]	90.0	20.3	45.0	0.4%	0.8%
CopperY-15	(1 1 1)[-1 –1 2]	90.0	50.3	45.0	1.3%	3.5%
CopperY-30	(3 2 3)[-1 3 –1]	202.7	50.0	57.0	1.4%	27.4%
CopperY+30	(1 1 15)[-15–15 2]	90.0	5.3	45.0	0.0%	2.0%
CopperZ-15	(1 1 2)[-2 -4 3]	75.0	35.3	45.0	0.7%	0.5%
CopperZ+15	(1 1 2)[-4 -2 3]	105.0	35.3	45.0	1.4%	0.3%
S____Y+30	(1 2 7)[15-11 1]	7.9	18.1	29.4	4.7%	1.8%
S____Y+15	(7 1 15)[-7-11 4]	43.0	24.9	81.9	7.0%	1.5%
S____Y-30	(10 7 10)[-6 10 -1]	185.0	49.1	54.6	2.5%	28.1%
S____Y-15	(10 7 10)[-3-10 10]	66.3	50.1	53.4	3.0%	8.1%
S____Z+15	(2 1 3)[-1 -1 1]	74.0	36.7	63.4	0.9%	7.4%
S____Z-15	(2 1 3)[-3-15 7]	44.0	36.7	63.4	5.2%	0.9%
Brass_Y+30	(1 1 2)[1 –1 0]	0.0	35.2	45.0	4.3%	1.5%
Brass_Y+15	(1 3 4)[12 –8 3]	20.1	37.9	20.1	25.8%	0.9%
Brass_Z+15	(0 1 1)[7 -6 6]	50.3	45.0	0.0	2.1%	0.6%
Brass_Z-15	(0 1 1)[15 -4 4]	20.3	45.0	0.0	0.7%	2.1%
Cube_____	(0 0 1)[1 0 0]	0.0	0.0	0.0	0.3%	0.1%
RD_Cube___	(0 1 2)[1 0 0]	0.0	26.6	0.0	2.9%	1.0%
TD_Cube___	(0 2 3)[0 -3 2]	90.0	33.7	0.0	18.1%	0.1%
ND_Cube___	(0 0 1)[-3 1 0]	198.4	0.0	0.0	1.4%	1.7%
Total					91.1%	92.9%

REFERENCES

[1] A. Morawiec, J.J. Fundenberger, E. Bouzy & J.S. Lecomte, J. Appl. Cryst. **35**, 287 (2002).

[2] J.J. Fundenberger, A. Morawiec, E. Bouzy, J.S. Lecomte, Mater. Chem. Phys. **81**, 535 (2003).

[3] J.J. Fundenberger, A. Morawiec, E. Bouzy & J.S. Lecomte, Ultramicroscopy **96**, 127 (2003).

[4] A. Morawiec, J. Appl. Cryst. **32**, 788 (1999).

[5] E-mail : lecomte@letam.sciences.univ-metz.fr Web : http://www.letam.sciences.univ-metz.fr

[6] J. Pospiech, K. Lücke, K. Sztwiertnia, Acta metall. mater. **41**, 305 (1993).

[7] R.A. Schwarzer, Ultramicroscopy **67**, 19 (1997).

[8] K. Sztwiertnia, F. Haessner, Mater. Sci. Forum **157-162**, 1069 (1994).

[9] K. Sztwiertnia, Mater. Sci. Forum **426 -432**, 3721 (2003).

[10] K. Sztwiertnia, J. Morgiel, E. Bouzy, Archives of Metall., 50, 119-130 (2005).

[11] J. Hansen, J. Pospiech, K. Lücke, Tables for Texture Analysis of Cubic Crystals, Springer-Verlag 1978.

[12] K. Sztwiertnia, J. Pospiech, F. Haessner, Texture Microstruct. **12**, 233 (1990).

Received: 10 June 2005.